



Influence of surface properties and sea ice thickness on light transmission

Christian Katlein¹, Stefanie Arndt¹, Marcel Nicolaus¹, Donald K. Perovich², Michael V. Jakuba³, Stefano Suman³, Stephen Elliott³, Louis L. Whitcomb^{3,4}, Christopher J. McFarland⁴, Rüdiger Gerdes¹, Antje Boetius^{1,5}, Christopher R. German³

Nereid Under-Ice, a new polar ROV

Increased light transmission leads to increased deposition of solar energy in the upper ocean and thus plays a crucial role in the amount and timing of sea-ice-melt and under-ice primary production. Recent developments in underwater technology provide new opportunities to undertake challenging research at the largely inaccessible underside of sea ice.

We measured spectral under-ice radiance and irradiance onboard the new Nereid Under-Ice (NUI) underwater robotic vehicle, during a cruise of the R/V Polarstern to 83°N 6°W in the Arctic Ocean in July 2014. NUI is a next generation hybrid remotely operated vehicle (H-ROV) designed for both remotely-piloted and autonomous surveys underneath land-fast and moving sea ice. Here we present results from one of the first comprehensive scientific dives of NUI employing its interdisciplinary sensor suite. We combine under-ice optical measurements with three-dimensional under-ice topography and aerial images of the surface conditions.

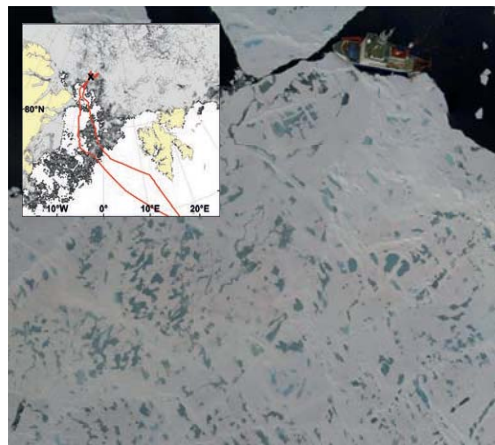


Figure 2: Mosaic of aerial images of the investigated ice field taken during a low altitude helicopter survey and used for albedo calculations. The length of Polarstern is 120m for reference. Inlay map shows the cruise track (red line) and the ice station position (black cross) off northeast Greenland.

Conclusions

- 72% of light variability can be explained by ice draft and surface albedo
- Averages over larger footprints better describe the variability
- Light field variability is governed by melt ponds on small scales (~100m) and by ice thickness/type on larger scales
- Spatially extensive datasets allow statistical treatment on the basis of histograms
- Histograms of under-ice light conditions can be inferred from distribution functions of albedo and ice thickness
- Geometric effects have to be considered in data interpretation underneath a heterogeneous ice cover

Length scales of variability

Variability length scales were derived from different subsets of the dataset by analysis of spatial variograms:

	Pole survey (~100m)	All data (~2km)
ice-draft	26.8m	15.1m
albedo	8.4m	10.6m
light transmission	8.4m	16.6m

Estimation of light histograms

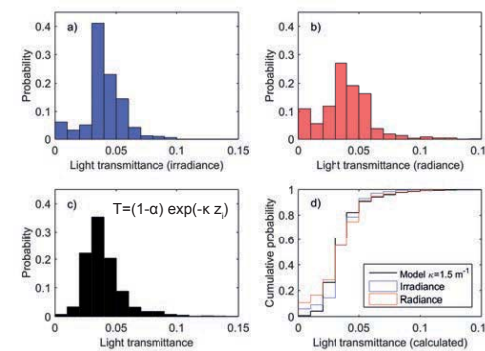


Figure 4: Histograms of light transmission as obtained from the irradiance (a) and radiance sensors (b). Light transmission histograms generated with the presented algorithm from the distribution of surface albedo and ice thickness using a bulk extinction coefficient of $\kappa = 1.5 \text{ m}^{-1}$ for the case of independent source distribution functions (c). Same histograms presented as cumulative probability functions (d).



Figure 1: The Nereid Under-Ice (NUI) H-ROV during deployment from R/V Polarstern. The vehicle has high bandwidth Ethernet connection to the ship via an unstructured optical fiber that spools off between the towbody (red) and the depressor (white, both visible in top of image) after separation under water. Upward looking sensors are located in the spine payload bay forward of the main lifting point.

Geometric effects under a heterogeneous sea ice cover

Arctic summer sea ice exhibits strong heterogeneity of optical properties on relatively short spatial scales. As the footprints of different radiometers are rather large, this heterogeneity causes geometric effects that need to be taken into account in the analysis of measured data.

This affects small scale lateral investigations, as well as vertical measurements where sensors are lowered through a hole in the ice. Derivation of inherent optical properties of the seawater can thus be erroneous in ice covered waters, if contamination by geometric effects is not avoided effectively.

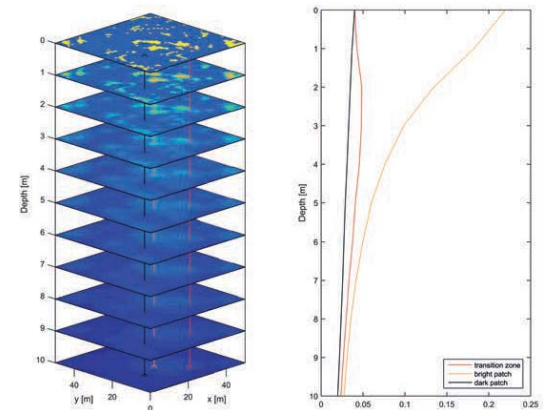


Figure 5: a) Depth slices of the light field underneath a surface geometry extracted from the aerial image (Figure 2) and idealized by classification into two transmittance classes. Bright colors show high light transmittance. b) Vertical irradiance profiles extracted from three different classifying locations indicated in a. Geometric effects are clearly visible in transition zone (red line).